The Pore Dimensions of Gramicidin A

Oliver S. Smart, Julia M. Goodfellow, and B. A. Wallace
Department of Crystallography, Birkbeck College, University of London, London WC1E 7HX, England

ABSTRACT The ion channel forming peptide gramicidin A adopts a number of distinct conformations in different environments. We have developed a new method to analyze and display the pore dimensions of ion channels. The procedure is applied to two x-ray crystal structures of gramicidin that adopt distinct antiparallel double helical dimer conformations and a nuclear magnetic resonance (NMR) structure for the $\beta^{6.3}$ NH_2-terminal to NH_2-terminal dimer. The results are discussed with reference to ion conductance properties and dependence of pore dimensions on the environment.

INTRODUCTION

Gramicidin A is a linear antibiotic peptide produced by *Bacillus brevis* (Hotchkiss and Dubos, 1940). Its primary sequence is HCO-L-Val-Gly-L-Ala-D-Leu-L-Ala-D-Val-L-Val-D-Val-(L-Trp-D-Leu)$_3$-L-Trp-$NHCH_2CH_2OH$ (Sarges and Witkop, 1965). Although the biologically significant role of gramicidin remains unclear (Harold and Baarda, 1967; Sarkar and Paulus, 1972; Paulus et al., 1979; Fisher and Blumenthal, 1982; Mandl and Paulus, 1985; Bohg and Ristow, 1986), its primary scientific interest lies in the ability of the peptide to form ion channels in lipid membranes (Andersen, 1984). The channels specifically conduct monovalent cations (alkali metals, Tl^+, Ag^+, NH_4^+ and H^+) (Myers and Haydon, 1972). The conducting species in lipid bilayers is known to be a dimer (Veatch and Stryer, 1977; Cifu et al., 1992).

The alternation of L and D-amino acids allows gramicidin to adopt forms of secondary structure that differ from allowed conformations in proteins. Structural models of gramicidin have been proposed based on NMR techniques (Arseniev et al., 1985; Chiu et al., 1991), model building (Urry, 1971; Ramachandran and Chandrasekaran, 1972; Veatch et al., 1974; Koeppe and Kimura, 1984), and x-ray crystallography (Wallace and Ravikumar, 1988; Langs, 1988; Langs et al., 1991). The major conducting species in lipid membranes is known to be a dimer of $\beta^{6.3}$ helices with the formyl-NH ends associated in the center of the membrane (Weinstein et al., 1980). Models of this structure were proposed by Urry (1971) and independently by Ramachandran and Chandrasekaran (1972). A 2D proton NMR study in a micellar environment by Arseniev et al. (1985) has produced an experimental structure for this form. This differs from the Urry structure in that the helices are right- rather than left-handed. The model is in broad accordance with solid-state NMR data obtained for gramicidin in the bilayer environment (Chui et al., 1991).

Three x-ray crystal structures of gramicidin have been reported with atomic resolution (Wallace and Ravikumar, 1988; Langs, 1988; Langs et al., 1991). All are antiparallel left-handed double helices. These forms have been designated "pores" to distinguish them from the "channel" structure discussed above (Wallace and Ravikumar, 1988). The structure reported by Wallace and Ravikumar (1988) was obtained from crystals of gramicidin grown from a solution of cesium chloride in methanol. The asymmetric unit contains two independent dimers of gramicidin (denoted here as copy 1 and copy 2). The double helix has a pitch of 6.4 residues per turn. Each pore is found to bind two cesium and three chloride ions. The structures determined by Langs and co-workers are determined from gramicidin crystals grown from ethanol (Langs, 1988), which adopts an orthorhombic morphology, and methanol (Langs et al., 1991) which takes up monoclinic geometry. Both structures are antiparallel double helices with 5.6 residues per turn. The forms differ principally in their side-chain orientations. No density for solvent molecules was observed in the pore of either ion-free molecule.

Reports of the atomic structures of gramicidin conformers have included values for the pore/channel radius or diameter. These generally have been based on interatomic distances across the channel, sometimes with the van der Waals radius of the atoms subtracted (Arseniev et al., 1985). Such figures are difficult to compare and do not convey information as to where constrictions in the channel occur. Visualization of the internal surface of a channel is also difficult. Representation by the van der Waals or solvent accessible surface (Connolly, 1983) is complicated by the presence of the external surface. The Connolly solvent accessible surface generation routine (Connolly, 1983) can produce cusp artifacts if the probe sphere radius is slightly larger than a constriction. Methods for the location and display of cavities on protein surfaces have recently been developed (Ho and Marshall, 1990; Levitt and Banaszak, 1992). Although these may be suitable to visualize the gramicidin pore, they may not be able to cope with tight twisting constrictions and do not provide information about the variation of pore radius along a channel. This paper presents a method that can provide both numerical information about, and allow the visualization of, the internal surface of an ion channel.

Received for publication 14 June 1993 and in final form 13 September 1993.
Address reprint requests to Dr. Oliver S. Smart, Department of Crystallography, Birkbeck College, University of London, Malet Street, London WC1E 7HX, England.
© 1993 by the Biophysical Society
0006-3495/93/12/2455/06 $2.00

MATERIALS AND METHODS

The procedure requires that the user specifies an initial point **p** that lies anywhere within the channel and a vector **v** that is approximately in the direction of the channel. Results were found to be only slightly sensitive to the values taken for these parameters. A sphere with radius $R(\mathbf{p})$ can be centered at **p** without overlapping any atom:

$$R(\mathbf{p}) = \min_{i=1}^{N_{atom}} [\,|\,\mathbf{x}_i - \mathbf{p}\,| - vdW_i], \quad (1)$$

where x is the vector giving the position of atom i and vdW_i is the van der Waals radius of the atom. The values used for the van der Waals radii were taken from AMBER (Weiner et al., 1984). Any ions or solvent molecules found in the channel are excluded from consideration. The Metropolis Monte Carlo simulated annealing procedure (Metropolis et al., 1953; Kirkpatrick et al., 1983) is used to adjust the point **p** to find the largest sphere whose center lies on the plane through the original point orthogonal to the channel vector **v**. New trial points on the plane, $\mathbf{p}_{new}$, are generated:

$$\mathbf{p}_{new} = \mathbf{p} + D\hat{\mathbf{y}}_{rand} \quad (2)$$

where D is a random number lying between zero and D_{max}, the user-specified maximum displacement, and the circumflex symbol (^) denotes a unit vector. The random vector $\mathbf{y}'_{rand}$ in the plane defined by **p** and **v** is generated from a three-dimensional random vector y_{rand}:

$$\mathbf{y}'_{rand} = \hat{\mathbf{y}}_{rand} - (\hat{\mathbf{v}} \cdot \hat{\mathbf{y}}_{rand})\hat{\mathbf{v}}. \quad (3)$$

If the change to the new point produces an increase in the accommodated sphere size, i.e., $R(p_{new}) > R(p)$, then the step is accepted and **p** is set to $\mathbf{p}_{new}$. On the other hand, if the sphere radius at the new point is smaller than that at the current point then the position $\mathbf{p}_{new}$ is accepted with the probability:

$$\exp\{[R(\mathbf{p}_{new}) - R(\mathbf{p})]/K\}. \quad (4)$$

The control constant K is analogous to the Boltzmann factor k_bT in a simulation of a physical process (Kirkpatrick et al., 1983). The process is repeated 1000 times with a reduction in the control constant, by a factor of 0.9, on each step. The final result of the procedure is the point on the initial plane at which the largest sphere can be accommodated. This point is stored and the process repeated after taking a small displacement d in the direction of the approximate channel vector **v** to find an optimal position to center a sphere on the new plane. The process is repeated on successive planes until the end of the channel/pore has been reached: when the accommodated sphere radius exceeds 5 Å. In turn, the whole process is restarted from the initially defined point in the direction –**v**. The net result of the routines is a series of sphere positions that can be thought of as the locus of a flexible sphere "squeezing" through the ion-channel.

The use of the Metropolis Monte Carlo simulated annealing procedure (Metropolis et al., 1953; Kirkpatrick et al., 1983) reduces the possibility of the routine becoming stuck in a local minimum. The maximum displacement D_{max} and initial control constant K are set to be as high as possible without causing the routine to jump through the pore/channel wall. The nondeterministic nature of the procedure does make results slightly run-dependent; however, this effect is not very significant (see below). It is also interesting to note that the procedure can work even if there is a constriction with no hole through it–the routine would converge to the point with the least van der Waals overlap and $R(p)$ would be negative.

Analysis of the pore/channel can be performed by plotting a graph of radius found versus the distance along the sphere center line. Visualization of the process is accomplished by producing a plot file that can be displayed in conjunction with the molecular structure using the programs HYDRA (Hubbard, 1986) or QUANTA (Molecular Simulations Inc., Waltham, MA 02154, USA).

The straightness of a channel/pore can be assessed by displaying a line connecting adjacent sphere centers. The internal surface of the pore is obtained by generating the locus of the outer surface of the sphere as it squeezes through the channel. This task is accomplished by considering dots at the surface of each sphere in the series except for the first and last centers. If a dot is within any other sphere, it is not displayed. In this manner, an irregular tube representation of the internal surface is obtained. Other visualization options (not presented here) aid the analysis of which atoms cause constrictions by joining each sphere surface with the closest two atoms, or the assessment of any deviations from a roughly cylindrical geometry by extending each dot drawn to a line terminating on contact with an atom's van der Waals surface.

The procedure has been implemented as a program HOLE written in standard FORTRAN-77. Random number generation uses the routine RAN0 given by Press et al. (1986). Source code is available free to any non-profit-making organization on request from the authors.

RESULTS AND DISCUSSION

The procedure has been applied to three experimentally determined structures of gramicidin A. The distance between planes d was set to 0.25 Å, the maximum displacement taken in a Monte Carlo step (D_{max}) to 0.3 Å and values taken for the control parameter (K) from 0.05 to 0.2 Å. Typical runs took about 4-min processor time on an IBM rs6000/220 work station. Co-ordinates for the antiparallel double helical pore conformation determined from crystals grown in ethanol (Langs, 1988) were obtained from the Protein Data Bank (Bernstein et al., 1977; Abola et al. 1987) at Brookhaven National Laboratory (entry 1GMA). This conformer ($\uparrow\downarrow \beta^{5,6}$) has a narrow irregular internal surface, Fig. 1.

In contrast, the hole through the structure determined with cesium and chloride in the pore (Wallace and Ravikumar, 1988) has a very much more regular structure. The x-ray structure has two independent dimers in the asymmetric unit

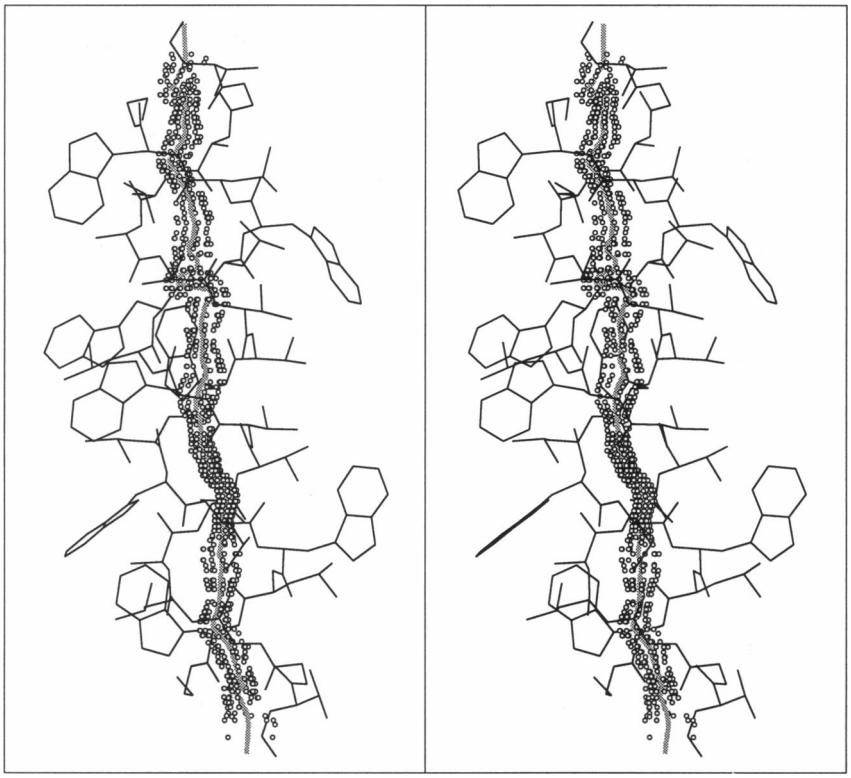

FIGURE 1 A stereographic picture of the internal surface of the $\uparrow\downarrow \beta^{5.6}$ structure of gramicidin A (Langs, 1988). The dots show the locus of the outer surface of a flexible sphere squeezing through the pore. The center line of the pore is shown in gray.

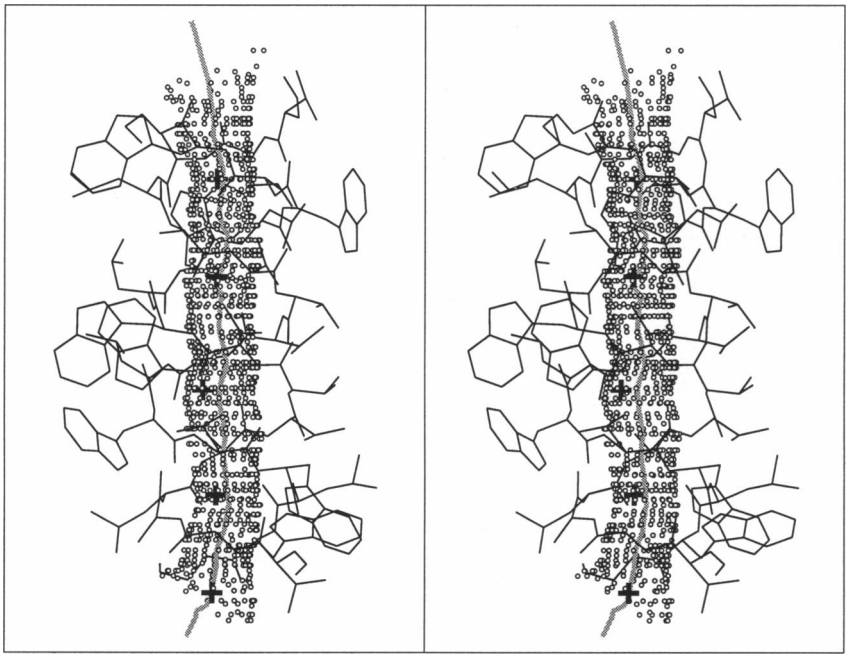

FIGURE 2 The internal surface of the $\uparrow\downarrow \beta^{6.4}$ conformer copy 1. Positions of cesium and chloride ions within the pore are marked by crosses. The scale used is the same as in Fig. 1 and subsequent figures.

(denoted here as $\uparrow\downarrow \beta^{6.4}$ copies 1 and 2). The internal surfaces of each of these forms are shown in Figs. 2 and 3.

The geometry of the channel ($\leftarrow\rightarrow \beta^{6.3}$) form was analyzed from coordinates kindly provided by Dr Benoît Roux (University of Montreal). These are the result of energy minimization from the structure determined with 2D proton NMR by Arseniev et al. (1985). The channel shape for this form is detailed in Fig. 4. The conformer shows constrictions at the entrance to the channel and a widening at the intermonomer junction.

Detailed comparison between the different forms is shown graphically in Fig. 5. In addition the "vital statistics" for each conformer are given as Table 1. Here the end point of a pore is defined as the first sphere center found whose radius is under 2 Å. The maximum pore radius is defined as the maximum value found between the two first minima within the pore.

The internal geometry of the two types of antiparallel double helical conformers are very different. The $\uparrow\downarrow \beta^{5.6}$ has a minimum pore radius of 0.42 Å and three wide places with

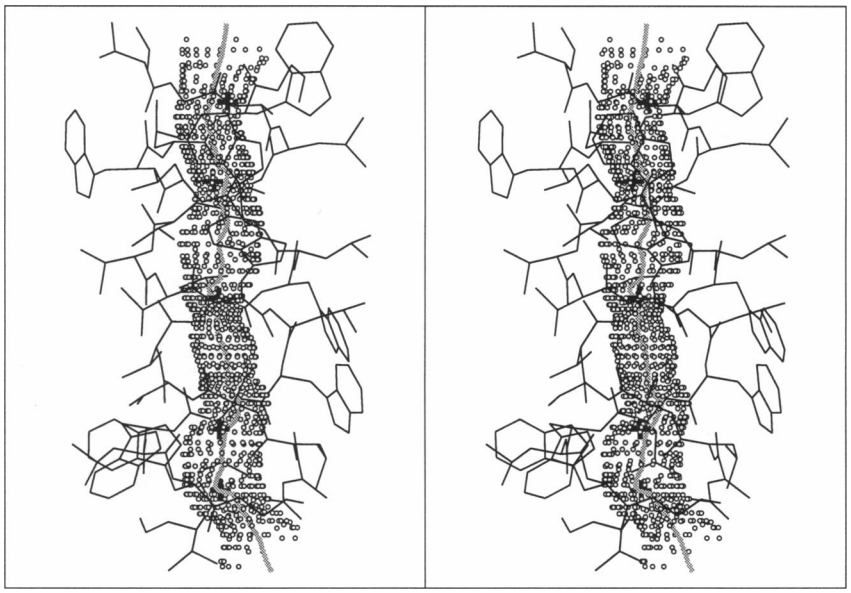

FIGURE 3 The internal surface of the $\uparrow\downarrow \beta^{6.4}$ conformer copy 2.

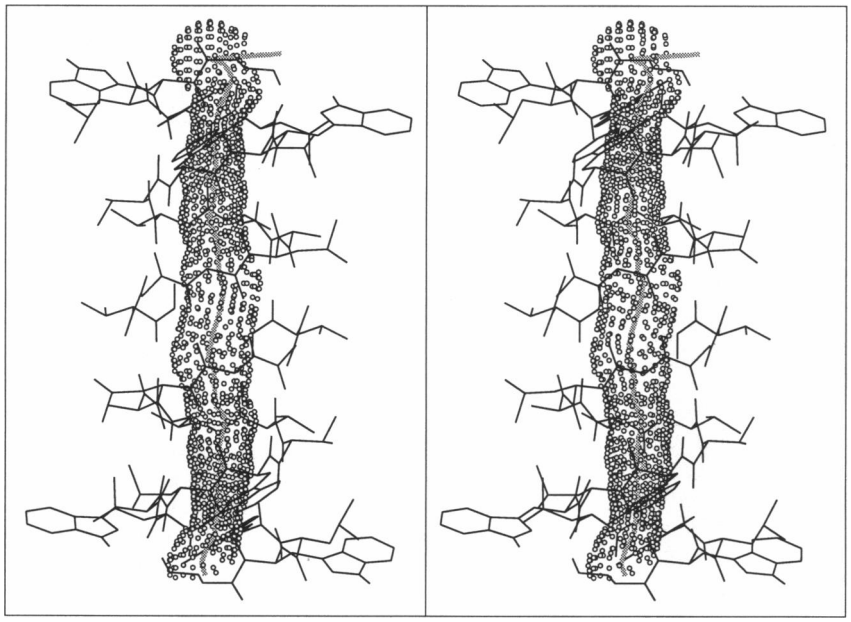

FIGURE 4 The internal surface of the $\leftarrow\rightarrow\beta^{6.3}$ channel structure.

radii of just under 1 Å (Table 1 and Fig. 5). This is insufficient to accommodate water molecules anywhere within the pore without rearrangements of backbone atoms: no indication of solvent in the pore was found in the experimental structure (Langs, 1988). However, it may be possible to accommodate small unsolvated ions (such as Li^+, ionic radius 0.60 Å) in the widest parts of the pore: differences in circular dichroism (CD) spectra of gramicidin A, in organic solvents, have been observed on binding Li^+ as opposed to Cs^+ (Wallace, 1987). Comparison of the internal cavity size of the $\uparrow\downarrow \beta^{5.6}$ form and that of an α-helix, with a radius that runs from 0.05 Å to 0.2 Å, shows that the structure is far from compact. In this context, it is interesting to note that Hodgkin (1949) gives data indicating dried gramicidin crystals grown from ethanol are less dense than dry crystals of either proteins or peptides.

The very different pore dimensions of the $\uparrow\downarrow \beta^{6.4}$ form accord with the observation of the change in the CD spectrum when cesium chloride is added to gramicidin in ethanolic solution (Wallace, 1984). Both cesium and chloride ions lie some distance from the pore center line (an average of 0.6 Å) and are not necessarily associated with bulges (Figs. 2, 3, and 5). This indicates that the presence of solvent molecules within the pore is probably the determinant of the internal cavity size. Electron density for solvent positions between the cesium and chloride ions is indicated by the X-ray data (Wallace and Ravikumar, 1988).

The two $\uparrow\downarrow \beta^{6.4}$ structures have different pore dimensions despite being in very similar environments (Fig. 5). The effect might be diminished with full structural refinement (B. A. Wallace and D. Doyle, in preparation). It may arise

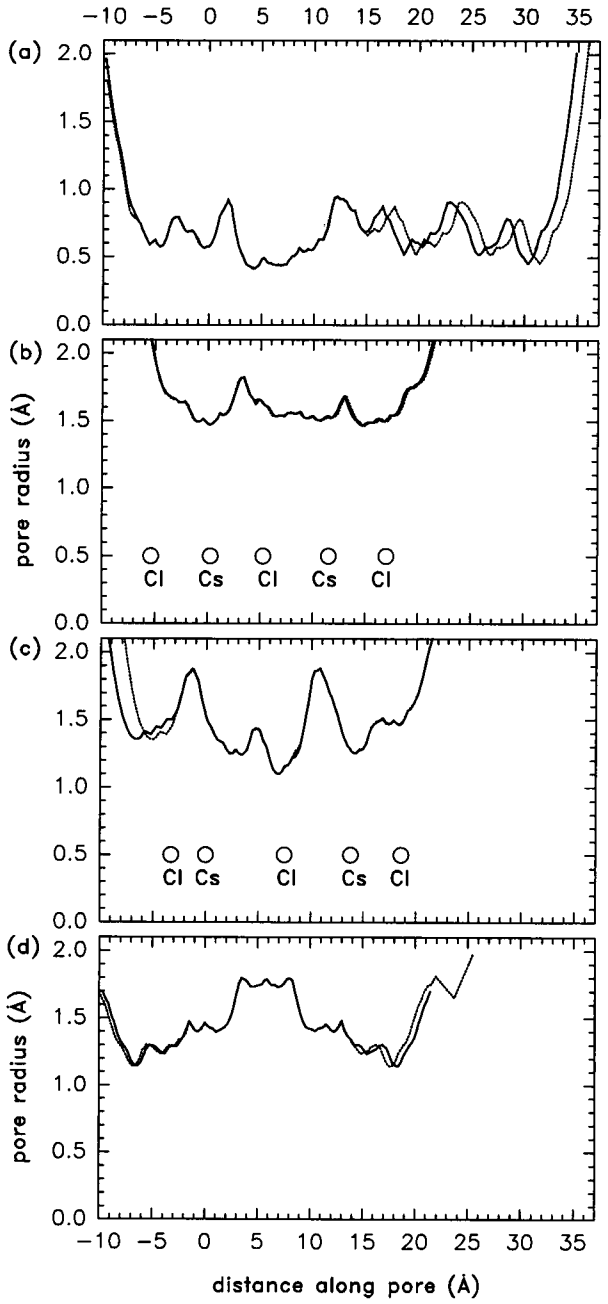

FIGURE 5 A graph showing the pore radius determined versus the distance along the pore center line, for: (*a*) The $\Uparrow\Downarrow \beta^{5.6}$ structure (*b*) $\Uparrow\Downarrow \beta^{6.4}$ conformer copy 1 (*c*) $\Uparrow\Downarrow \beta^{6.4}$ conformer copy 2 (*d*) $\longleftrightarrow \beta^{6.3}$ channel structure. In each case the result of two runs are shown in dotted and solid lines. In (*b*) and (*c*) the ion positions indicated are the positions of each ions closest approach to the sphere center.

due to variations in crystal contacts but is more likely to be due to differences in the ion binding sites of the two dimers. The less regular structure of the second copy could be due to the fact that the cesium and chloride ions are closer in that structure causing disruption of the main chain.

The pore dimensions of the $\Uparrow\Downarrow \beta^{6.4}$ and $\leftarrow\rightarrow \beta^{6.3}$ forms are quite similar (Table 1). This lends credence to the speculative identification of antiparallel double helical pore as being a long-lived minor conducting species in lipid bilayers

TABLE 1 Pore dimensions determined*

Form	$\Uparrow\Downarrow \beta^{5.6}$	$\Uparrow\Downarrow \beta^{6.4}$ Copy 1	$\Uparrow\Downarrow \beta^{6.4}$ Copy 2	$\leftarrow\rightarrow$ $\beta^{6.3}$
Minimum pore radius†	0.42 (0.69)	1.46 (1.91)	1.10 (1.56)	1.14 (1.41)
Maximum pore radius†	0.95 (1.38)	1.82 (2.22)	1.88 (2.24)	1.80 (2.16)
Distance between pore ends	35	24	24	25
Distance along pore	~45	~26	~28	~32

* All values in Ångstrom units (1 Å = 10^{-10}m).

† The first value is calculated using the van der Waals radii (Weiner et al., 1984), whereas the figure in brackets uses hard core radii (Turano et al., 1992).

(Durkin, 1986), and the observation that mutants of gramicidin are able to form long-lived conducting species that do not have a $\leftarrow\rightarrow \beta^{6.3}$ structure (Durkin et al., 1987; Koeppe et al., 1991).

It is interesting to consider how the 1.14 Å constriction found in the $\leftarrow\rightarrow \beta^{6.3}$ structure (Table 1) accords with the ability of the channel to conduct ions larger than this. Indeed, the permeability of cesium, (ionic radius 1.67 Å) is higher than for smaller alkali ions (Myers and Haydon, 1972) and the channel conducts some even larger organic cations (Seoh and Busath, 1993). The simple comparison between the pore radius determined here and the ionic radius is misleading. The peak in the oxygen radial distribution function for a cesium ion in water occurs at 3.10 Å (Åqvist, 1990). Subtracting the value for the van der Waals radius of an oxygen atom (1.6 Å) results in an "effective radius" of 1.5 Å for the cesium ion. This accords with the observation that three of the four cesium ions in the $\Uparrow\Downarrow \beta^{6.4}$ structures marked in Fig. 5 occur at this pore radius. An effective radius of 1.5 Å is still larger than the size of the constriction. Part of the effect could be due to the fact that as the channel structure is determined using NMR data the backbone geometry and thus the pore dimensions may not be precisely defined as in the crystal structures. However, ion movement in the channel almost certainly causes changes to the channel geometry. Much more complex methods are needed to model such dynamic effects (Åqvist and Warshel, 1989; Jordan, 1990; Turano et al. 1992; Roux and Karplus, 1993). However, an approximate implicit treatment can be made by applying the procedure used here with "hard core" atomic radii (Turano et al., 1992) rather than the van der Waals radii. Hard core radii are variants of the van der Waals radii reduced to take into account overlaps caused by thermal motion. The minimum pore radius of the $\leftarrow\rightarrow \beta^{6.3}$ form calculated using these parameters is 1.41 Å (Table 1), reasonably close to the reduced radius for the cesium ion. It is interesting to note that Turano et al. (1992) find a energy barrier for the passage of a guanidinium ion through the channel at approximately 11 Å from the channel center. The constriction in the channel found here is in the same position (Fig. 5).

In conclusion, the examination of pore dimensions is a useful aid in the analysis of conformation and structure activity relations for ion channels. With our new method we

have been able to visualize the cavity and provide quantitative data on this important factor in the function of the polypeptide. Work in progress seeks to extend the analysis to other ion channel forming proteins.

We thank the UK Science and Engineering Research Council for support under project grant GR/G49494 and the Molecular Recognition and Computational Science Initiatives.

REFERENCES

Abola, E. E., F. C. Bernstein, S. H. Bryant, T. F. Koetzle, and J. Weng. 1987. Protein data bank. *In* Crystallographic Databases—Information Content, Software Systems, Scientific Applications. F. H. Allen, G. Bergerhoff, and R. Sievers, editors. Data Commission of the International Union of Crystallography, Bonn/Cambridge/Chester. 107–132.

Andersen, O. S. 1984. Gramicidin channels. *Annu. Rev. Physiol.* 46: 531–548.

Åqvist, J. 1990. Ion-water interaction potentials derived from free energy perturbation simulations. *J. Phys. Chem.* 94:8021–8024.

Åqvist, J., and A. Warshel. 1989. Energetics of ion permeation through membrane channels. Solvation of Na^+ by gramicidin A. *Biophys. J.* 56: 171–182.

Arseniev, A. S., I. L. Barsukov, V. F. Bystrov, A. L. Lomize, and Yu. A. Ovchinnikov. 1985. ^{1}H-NMR study of gramicidin A transmembrane ion channel: head-to-head right-handed, single-stranded helices. *FEBS Lett.* 186:168–174.

Bernstein, F. C., T. F. Koetzle, G. J. B. Williams, E. F. Meyer Jr., M. D. Brice, J. R. Rodgers, O. Kennard, T. Shimanouchi, and M. Tasumi. 1977. The Protein Data Bank: A computer-based archival file for macromolecular structures. *J. Mol. Biol.* 112:535–542.

Bohg, A., and H. Ristow. 1986. DNA-supercoiling is affected in vitro by the peptide antibiotics tyrocidine and gramicidin. *Eur. J. Biochem.* 160: 587–591.

Chiu, S-W., L. K. Nicholson, M. T. Brenneman, S. Subramanian, Q. Teng, J. A. McCammon, T. A. Cross, and E. Jakobsson. 1991. Molecular dynamics computations and solid state nuclear magnetic resonance of the gramicidin cation channel. *Biophys. J.* 60:974–978.

Cifu, A. S., R. E. Koeppe II, and O. S. Andersen. 1992. On the supramolecular organization of gramicidin channels. The elementary conducting unit is a dimer. *Biophys. J.* 61:189–203.

Connolly, M. L. 1983. Solvent-accessible surfaces of proteins and nucleic acids. *Science (Washington DC).* 221:709–713.

Durkin, J. T. 1986. Discussion comment. *Biophys. J.* 49:306.

Durkin, J. T., O. S. Andersen, F. Heitz, J. Trudelle, and R. E. Koeppe II. 1987. Linear gramicidins can form channels that do not have the $\beta^{6.3}$ structure. *Biophys. J.* 51:451a.

Fisher, R., and T. Blumenthal. 1982. An interaction between gramicidin and the σ subunit of RNA polymerase. *Proc. Natl. Acad. Sci. USA.* 79: 1045–1048.

Harold, F. M., and J. R. Baarda. 1967. Gramicidin, valinomycin, and cation permeability of *Streptococcus faecalis*. *J. Bacteriol.* 94:53–60.

Ho, C. M. W., and G. R. Marshall. 1990. Cavity search: An algorithm for the isolation and display of cavity-like binding regions. *J. Computer-Aided Mol. Design.* 4:337–354.

Hodgkin, D. C. 1949. X-ray analysis and protein structure. *Cold Spring Harbor Symp. Quant. Biol.* 14:65–78.

Hotchkiss, R. D., and R. J. Dubos. 1940. Fractionation of the bactericidal agent from cultures of a soil bacillus. *J. Biol. Chem.* 132:791–792

Hubbard, R. E. 1986. HYDRA: current and future developments. *In* Computer Graphics and Molecular Modeling. R. Fletterick and M. Zoller, editors. Cold Spring Harbor Laboratory, Cold Spring Harbor, NY. 9–11.

Jordan, P. C. 1990. Ion-water and ion-polypeptide correlations in a gramicidin-like channel. A molecular dynamics study. *Biophys. J.* 58: 133–1156.

Kirkpatrick, S., C. D. Gelatt Jr., and M. P. Vecchi. 1983. Optimization by simulated annealing. *Science (Washington DC).* 220:671–680.

Koeppe, R. E. II, and M. Kimura. 1984. Computer building of β-helical polypeptide model. *Biopolymers.* 23:23–38.

Koeppe, R. E., II, D. V. Greathouse, L. L. Providence, and O. S. Andersen. 1991. [L-Leu^9-D-Trp^{10}-L-Leu^{11}-D-Trp^{12}-L-Leu^{13}-D-Trp^{14}-L-Leu^{15}]gramicidin forms both single- and double-helical channels. *Biophys. J.* 59: 319a.

Langs, D. A. 1988. Three-dimensional structure at 0:86 Å of the uncomplexed form of the transmembrane ion channel peptide gramicidin A. *Science (Washington DC).* 241:188–191.

Langs, D. A., G. D. Smith, C. Courseille, G. Précigoux, and M. Hospital. 1991. Monoclinic uncomplexed double-stranded, antiparallel, left handed $\beta^{5.6}$-helix ($\beta^{5.6}$) structure of gramicidin A: Alternate patterns of helical association and deformation. *Proc. Natl. Acad. Sci. USA.* 88:5345–5349.

Levitt, D. G., and L. J. Banaszak. 1992. POCKET: A computer graphics method for identifying and displaying protein cavities and their surrounding amino acids. *J. Mol. Graphics.* 10:229–234.

Mandl, J., and H. Paulus. 1985. Effect of linear gramicidin on sporulation and intracellular ATP pools of *Bacillus brevis*. *Arch. Microbiol.* 143: 248–252.

Metropolis, N., A. W. Rosenbluth, M. N. Rosenbluth, A. H. Teller, and E. Teller. 1953. Equation of state calculations by fast computing machines. *J. Chem. Phys.* 21:1087–1092.

Myers, V. B., and D. A. Haydon. 1972. Ion transfer across lipid membranes in the presence of gramicidin A. II. The ion selectivity. *Biochim. Biophys. Acta.* 274:313–322.

Paulus, H., N. Sarkar, P. K. Mukherjee, D. Langley, V. T. Ivanov, E. N. Shepel, and W. Veatch. 1979. Comparison of the effect of linear gramicidin analogues on bacterial sporulation, membrane permeability, and ribonucleic acid polymerase. *Biochemistry.* 18:4532–4536.

Press, W. H., B. P. Flannery, S. A. Teukolsky, and W. T. Vetterling. 1986. Numerical Recipes, The Art of Scientific Computing. Cambridge University Press, Cambridge. 194–195.

Ramachandran, G. N., and R. Chandrasekaran. 1972. Conformation of peptide chains containing both L- & D-residues: Part I - helical structures with alternating L- & D-residues with special reference to the LD-ribbon & the LD-helices. *Indian J. Biochem. Biophys.* 9:1–11.

Roux, B., and M. Karplus. 1993. Ion transport in the gramicidin channel: free energy of the solvated right-handed dimer in a model membrane. *J. Am. Chem. Soc.* 115:3250–3262.

Sarges, R., and B. Witkop. 1965. Gramicidin A. V. The structure of valine- and isoleucine-gramicidin A. *J. Am. Chem. Soc.* 87:2011–2020.

Sarkar, N., and H. Paulus. 1972. Function of peptide antibiotics in sporulation. *Nature New Biol.* 239:228–230.

Seoh, S.-A., and D. Busath. 1993. The permeation properties of small organic cations in gramicidin A channels. *Biophys. J.* 64:1017–1028.

Turano, B., M. Pear, and D. Busath. 1992. Gramicidin channel selectivity. Molecular mechanics calculations for formamidinium, guanidium, and acetamidinium. *Biophys. J.* 63:152–161.

Urry, D. W. 1971. The gramicidin A transmembrane channel: A proposed π(L, D) helix. *Proc. Natl. Acad. Sci. USA.* 68:672–676.

Veatch, W. R., E. T. Fossel, and E. R. Blout. 1974. The conformation of gramicidin A. *J. Am. Chem. Soc.* 13:5249–5256.

Veatch, W., and L. Stryer. 1977. The dimeric nature of the gramicidin A transmembrane channel: Conductance and fluoresence energy transfer studies of hybrid channels. *J. Mol. Biol.* 113:89–102.

Wallace, B. A. 1984. Ion-bound forms of the gramicidin A transmembrane channel. *Biophys. J.* 45:114–116.

Wallace, B. A. 1987. The structure of gramicidin, a transmembrane ion channel. *In* Ion Transport Through Membranes. K. Yagi and B. Pullman, editors. Academic Press, Tokyo. 255–275.

Wallace, B. A., and K. Ravikumar. 1988. The gramicidin pore: crystal structure of a cesium complex. *Science (Washington DC).* 241:182–187.

Weiner, S. J., P. A. Kollman, D. A. Case, U. C. Singh, C. Ghio, G. Alagona, S. Jr. Profeta, and P. Weiner. 1984. A new force field for molecular mechanical simulation of nucleic acids and proteins. *J. Am. Chem. Soc.* 106:765–784.

Weinstein, S., B. A. Wallace, J. S. Morrow, and W. R. Veatch. 1980. Conformation of the gramicidin A transmembrane channel: A ^{13}C nuclear magnetic resonance study of ^{13}C-enriched gramicidin in phosphatidylcholine vesicles. *J. Mol. Biol.* 143:1–19.